

**CRYSTAL ENGINEERING OF AZOLATE-BASED FRAMEWORKS:  
SYNTHESIS AND STRUCTURAL CHEMISTRY**

**MANISHA JADON**



**DEPARTMENT OF CHEMISTRY**

**INDIAN INSTITUTE OF TECHNOLOGY DELHI**

**FEBRUARY 2023**

**©Indian Institute of Technology Delhi (IITD), New Delhi, 2023**

**CRYSTAL ENGINEERING OF AZOLATE-BASED FRAMEWORKS:  
SYNTHESIS AND STRUCTURAL CHEMISTRY**

by

**Manisha Jadon**

**Department of Chemistry**

*Submitted*

*in fulfilment of the requirement of the degree of Doctor of philosophy*

*to the*



**INDIAN INSTITUTE OF TECHNOLOGY DELHI**

**FEBRUARY 2023**

*Dedicated to*

*my husband and my parents*

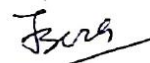
## CERTIFICATE

This is to certify that the thesis entitled, “Crystal engineering of azolate-based frameworks: Synthesis and structural chemistry”. Being submitted by Ms. Manisha Jadon to the Indian Institute of Technology Delhi and Indian Oil Corporation Limited, Faridabad for the award of the degree of **Doctor of Philosophy** in Chemistry, is a record of bonafide research work carried out by her. Ms. Manisha Jadon has worked under our guidance and supervision and has fulfilled the requirements for the submission of this thesis, which to my knowledge has reached the requisite standard.

The results contained in this dissertation have not been submitted, in part or full, to any other university or institute for award of any degree or diploma.



Prof. A. RAMANAN  
Supervisor  
Department of Chemistry  
Indian Institute of Technology Delhi  
New Delhi – 110016



Dr. TAPAN BERA  
Co-supervisor  
Department of Alternate Energy  
Indian Oil Corporation Limited  
Faridabad (Haryana) – 121007

डॉ. तपन बेरा / Dr. Tapan Bera  
एन. गवर्नर (डिप्लोमेटिक रजि.) / Dy. General Manager (Alternate Energy)  
इंडियन ऑयल कॉर्पोरेशन लिमिटेड  
Indian Oil Corporation Limited  
अनुसंधान एवं विकास केंद्र / R&D Centre  
सेक्टर-13, फरीदाबाद-121007, हरियाणा (भारत)  
Sector-13, Faridabad-121007, Haryana (India)

## ACKNOWLEDGEMENTS

I express my deep sense of gratitude and profound thanks to my supervisor Prof. A. Ramanan. Throughout my Ph.D, he created a friendly research atmosphere for me, enlightened me with great ideas. It was really a lifetime experience for me to work with him. I wish to express my sincere thanks to Dr. Tapan Bera, for his valuable discussion and support throughout my Ph.D work at IIT Delhi. I would like to thank present and former heads of the Department of Chemistry and faculty members for their help and cooperation. I would also like to thank all the staff associated with the Department of Chemistry, IIT Delhi.

I am grateful to CSIR, New Delhi and IOCL, Faridabad for providing fellowship support. I thank IIT Delhi and DST & SERB for providing instrumentation and other infrastructure facilities.

The journey of research became easy with the support of Dr. Bhawna Singh, Dr. Bhawna Uttam, Dr. Arun Patel, Dr. Pradeep Kumar Jangra, Dr. Ravi Teja, Sahil Singh, Prabuddhkant Mishra, and Archismati Dubey. I would like to thank my seniors Dr. Pramod Kumar, Dr. Manju Srivastava, Dr. Vineet Kumar, Dr. Balendra, for their guidance and help. I would also like to thank my labmates Bharti Singh and Shailabh Tewari for all the valuable discussions and creating friendly research atmosphere in the lab. My stay in the campus became memorable with Sakshi Katyal, Shweta Kaushik, Dr. Manisha Lamba, Dr. Bhawna Singh, Dr. Dipika, Deepa Bharadwaj and Shreya Tripathi. Their friendship, care and support are precious to me.

I would like to thank my husband who motivated me to complete my higher education and pursue PhD, for being there at every stage, guiding and helping me in cultivating patience and perseverance to endure challenges in life. I am grateful to my parents for letting me pursue my dreams. The unconditional love and support of my mother throughout my career and life,

especially during the last two years of PhD have made this day possible. The love and support of my husband and the blessings of my parents have made me what I am today. I owe everything to them. Dedicating this thesis to them is a minor recognition to their boundless affection.

## **Abstract**

The thesis entitled ‘Crystal Engineering of Azolate-based Frameworks: Synthesis and Structural Chemistry’ is focused on understanding the nucleation of crystals grown from solution. Today’s analytical techniques are not capable enough to study this phenomenon. Our objective is to understand the underlying mechanism of the formation of MOFs and utilize it to engineer new MOFs with desired properties. Yaghi’s work on MOFs is unprecedented in the design and synthesis of new porous solids. His SBU approach and topological considerations or reticular chemistry has provided greater insights towards engineering new targeted MOFs, though it is still difficult to predict the outcome of any crystallization reaction. Note, the SBU approach lacks molecular insights towards understanding nucleation of a crystal.

Crystallization is a supramolecular reaction. Supramolecular interactions involve all non-covalent interactions though H-bonding and coordination interactions dominate in most of the cases. Monitoring crystallization on a real time scale, especially at supersaturation involving relatively small number of molecules, calls for advanced imaging and spectroscopic techniques supported by logical theoretical models. Nucleation of a crystal is still a poorly understood phenomenon. Present day techniques used to study and understand the nucleation of a crystal are not efficient enough to access the size of critical nucleus ( $< 1\text{nm}$ ) and its periodic structure which falls in the range of a few thousands of molecules. It is difficult to know how a system chooses a specific pathway in the supersaturated solution from aggregating molecules to form a crystal nucleus. In this context, retrosynthetic analysis is a useful methodology to hypothesize a liquid like structure for this state. Retrosynthetic approach provides a link between aggregation in the solution and the solid-state structure observable by diffraction techniques. Here, we have adopted the retrosynthetic analysis to rationalise the crystal structures of related solids in a particular

system available in the structural database. The approach provides better picture of nucleation phenomenon of crystals growing from a solvent. (Chapter I)

Retrosynthetic analysis of the crystal structures revealed how the structural landscape of the different systems could be readily interpreted in terms of supramolecular aggregation between soluble molecular species present in the solution to facilitate the favorable interaction forming multidimensional coordination networks. First, we analyzed zinc–benzene dicarboxylate (BDC) system and showed how 1:1 Zn:BDC complex supramolecularly aggregates among themselves or with other ion pairs present in the solution under different reaction condition to finally result in a particular assembly (Chapter II). We extended this analysis to zinc imidazole dicarboxylate system and provided an experiment as a proof of concept to synthesize new solids (Chapter III). We succeeded in crystallizing one-dimensional zig-zag chains though our focus was to engineer new three-dimensional MOFs for gas storage applications. We opted for triazole instead of imidazole as the former showed a better tendency to form higher dimensional structures. This approach proved to be useful as we have successfully synthesized thirteen new three-dimensional cadmium triazolate polycarboxylates (Chapter IV). In Chapter V, a database analysis of another system, i.e., cobalt triazolate di/tricarboxylates led to the isolation of three new solids. we have also reported some preliminary studies on magnetism and hydrogen adsorption of **IITD-27**. In Chapter VI, we have summarized the significant results obtained in this study and the conclusions drawn from the overall investigation. The chapter also provides future scope of the work.

## अमूर्त

क्रिस्टल इंजीनियरिंग ऑफ़ एज़ोलेट-बेस्ड फ्रेमवर्क: सिंथेसिस एंड स्ट्रक्चरल केमिस्ट्री' शीर्षक वाली थीसिस समाधान से उगाए गए क्रिस्टल के न्यूक्लियेशन को समझने पर केंद्रित है। आज की विश्लेषणात्मक तकनीकें इस परिघटना का अध्ययन करने में पर्याप्त सक्षम नहीं हैं। हमारा उद्देश्य एमओएफ के गठन के अंतर्निहित तंत्र को समझना और वांछित गुणों के साथ नए एमओएफ को इंजीनियर करने के लिए इसका उपयोग करना है। एमओएफ पर याघी का काम नए झरझरा ठोस पदार्थों के डिजाइन और संश्लेषण में अभूतपूर्व है। उनके एसबीयू दृष्टिकोण और टोपोलॉजिकल विचार या रेटिकुलर केमिस्ट्री ने इंजीनियरिंग के नए लक्षित एमओएफ के प्रति अधिक अंतर्दृष्टि प्रदान की है, हालांकि किसी भी क्रिस्टलीकरण प्रतिक्रिया के परिणाम की भविष्यवाणी करना अभी भी मुश्किल है। ध्यान दें, एसबीयू दृष्टिकोण में क्रिस्टल के न्यूक्लियेशन को समझने की दिशा में आणविक अंतर्दृष्टि का अभाव है।

क्रिस्टलीकरण एक अतिआणविक अभिक्रिया है। सुपरमॉलेक्यूलर इंटरैक्शन में सभी गैर-सहसंयोजक इंटरैक्शन शामिल होते हैं, हालांकि अधिकांश मामलों में एच-बॉन्डिंग और समन्वय इंटरैक्शन हावी होते हैं। वास्तविक समय के पैमाने पर क्रिस्टलीकरण की निगरानी करना, विशेष रूप से अपेक्षाकृत कम संख्या में अणुओं को शामिल करने वाले सुपरसेटेशन पर, उन्नत इमेजिंग और स्पेक्ट्रोस्कोपिक तकनीकों के लिए तार्किक सैद्धांतिक मॉडल द्वारा समर्थित है। एक क्रिस्टल का न्यूक्लियेशन अभी भी एक खराब समझी जाने वाली घटना है। क्रिस्टल के न्यूक्लियेशन का अध्ययन करने और समझने के लिए उपयोग की जाने वाली वर्तमान तकनीकें महत्वपूर्ण नाभिक के आकार ( $<1\text{nm}$ ) और इसकी आवधिक संरचना तक पहुँचने के लिए पर्याप्त कुशल नहीं हैं जो कुछ हजारों अणुओं की सीमा में आती हैं। यह जानना मुश्किल है कि कैसे एक सिस्टम क्रिस्टल न्यूक्लियस बनाने के लिए एकत्रित अणुओं से सुपरसैचुरेटेड समाधान में एक विशिष्ट मार्ग चुनता है।

इस संदर्भ में, इस राज्य के लिए तरल जैसी संरचना की परिकल्पना करने के लिए रेट्रोसिंथेटिक विश्लेषण एक उपयोगी पद्धति है। रेट्रोसिंथेटिक दृष्टिकोण समाधान में एकत्रीकरण और विवर्तन तकनीकों द्वारा देखे जाने योग्य ठोस-अवस्था संरचना के बीच एक कड़ी प्रदान करता है। यहाँ, हमने संरचनात्मक डेटाबेस में उपलब्ध एक विशेष प्रणाली में संबंधित ठोस पदार्थों के क्रिस्टल संरचनाओं को युक्तिसंगत बनाने के लिए पूर्व-संश्लेषण विश्लेषण को अपनाया है। दृष्टिकोण एक विलायक से बढ़ने वाले क्रिस्टल की न्यूक्लियेशन घटना की बेहतर तस्वीर प्रदान करता है। (अध्याय 1)

क्रिस्टल संरचनाओं के रेट्रोसिंथेटिक विश्लेषण से पता चला कि कैसे विभिन्न प्रणालियों के संरचनात्मक परिदृश्य को समाधान में मौजूद घुलनशील आणविक प्रजातियों के बीच सुपरमॉलेक्यूलर एकत्रीकरण के संदर्भ में आसानी से व्याख्या की जा सकती है ताकि बहुआयामी समन्वय नेटवर्क बनाने के लिए अनुकूल बातचीत की सुविधा मिल सके। सबसे पहले, हमने जिंक-बेंजीन डाइकार्बोक्सिलेट (BDC) प्रणाली का विश्लेषण किया और दिखाया कि कैसे 1:1 Zn: BDC कॉम्प्लेक्स सुपरमॉलेक्यूलरली आपस में या अलग-अलग रिएक्शन कंडीशन के तहत सॉल्यूशन में मौजूद अन्य आयन जोड़े के साथ मिलकर एक विशेष असेंबली में परिणत होता है (अध्याय 2)। हमने इस विश्लेषण को जिंक इमिडाज़ोल डाइकार्बोक्सिलेट सिस्टम तक बढ़ाया और नए ठोस पदार्थों को संश्लेषित करने के लिए अवधारणा के प्रमाण के रूप में एक प्रयोग प्रदान किया (अध्याय 3)। हम एक-आयामी टेढ़ी-मेढ़ी जंजीरों को सघन बनाने में सफल रहे, हालांकि हमारा ध्यान गैस भंडारण अनुप्रयोगों के लिए नए त्रि-आयामी एमओएफ तैयार करने पर था। हमने इमिडाज़ोल के बजाय ट्राइज़ोल का विकल्प चुना क्योंकि पूर्व में उच्च आयामी संरचनाएँ बनाने की बेहतर प्रवृत्ति दिखाई दी।

यह दृष्टिकोण उपयोगी साबित हुआ क्योंकि हमने तेरह नए त्रि-आयामी कैडमियम ट्रायज़ोलेट पॉलीकार्बोक्सिलेट्स को सफलतापूर्वक संश्लेषित किया है (अध्याय 4)। अध्याय 5 में, एक अन्य प्रणाली के एक डेटाबेस विश्लेषण, यानी, कोबाल्ट ट्रायज़ोलेट डी/ट्राइकार्बोक्सिलेट्स ने तीन नए ठोस पदार्थों को अलग कर दिया। हमने IITD-27 के चुंबकत्व और हाइड्रोजन सोखने पर कुछ प्रारंभिक अध्ययनों की भी सूचना दी है। अध्याय 6 में, हमने इस अध्ययन में प्राप्त महत्वपूर्ण परिणामों और समग्र जांच से निकाले गए निष्कर्षों को संक्षेप में प्रस्तुत किया है। अध्याय कार्य के भविष्य के दायरे को भी प्रदान करता है।

## Table of Contents

<b>CERTIFICATE .....</b>	<b>(i)</b>
<b>ACKNOWLEDGEMENTS .....</b>	<b>(ii)</b>
<b>ABSTRACT .....</b>	<b>(iv)</b>
<b>Table of Contents .....</b>	<b>(viii)</b>
<b>List of Figures .....</b>	<b>(xiii)</b>
<b>List of Tables .....</b>	<b>(xxvi)</b>
<b>List of Schemes .....</b>	<b>(xxviii)</b>
<b>Abbreviations .....</b>	<b>(xxix)</b>
<b>Color codes of atoms or ligands .....</b>	<b>(xxxii)</b>
<b>Chapter I</b>	
<b>Introduction .....</b>	<b>(1-42)</b>
I.1 Supramolecular chemistry .....	3
I.2 Supramolecular or noncovalent interactions .....	5
I.3 Crystal synthesis .....	8
I.4 Crystal engineering .....	12
I.5 Metal-organic frameworks (MOFs) versus coordination polymers (CPs) .....	15
I.6 Reticular Chemistry: Engineering MOFs with desired topology .....	17

I.7 Designing MOFs for targeted applications .....	21
I.8 Commercialization of MOFs .....	25
I.9 Research gaps and motivation of the present work .....	26
References .....	30

## **Chapter II**

<b>From molecules to materials: Structural landscape of zinc terephthalates grown from solution .....</b>	<b>(43-81)</b>
II.1 Introduction .....	45
II.2 Summary and Conclusions .....	73
References .....	76

## **Chapter III**

<b>Structural landscape of zinc imidazole dicarboxylates– A crystal engineering strategy for the synthesis of 1D coordination polymer .....</b>	<b>(82-130)</b>
III.1 Introduction .....	84
III.2 Materials and methods .....	104
III.3 Experimental section .....	106
III.3.1 Synthesis .....	106
III.4 Results and discussion .....	108

III.4.1 Structural chemistry and crystal structures of the solids **IITD-1** to **IITD-8** .....108

III.5 Summary and conclusions .....127

References .....128

## **Chapter IV**

### **Crystal engineering of three-dimensional cadmium triazolate dicarboxylate based MOFs**

..... (131-216)

IV.1 Introduction .....133

IV.2 Materials and methods ..... 149

IV.3 Experimental section ..... 151

IV.3.1 Synthesis of single crystals of the solids– **IITD-9** to **IITD-24** and bulk samples of three-dimensional monophasic compounds .....151

IV.4 Results and discussion .....157

IV.4.1 Structural chemistry and crystal structures of the solids **IITD-9** to **IITD-24** .....167

IV.4.2 Thermal behaviour of the solids– **IITD-9** to **IITD-24** .....190

IV.4.3 ATR and FTIR analysis of the solids– **IITD-9** to **IITD-24** .....195

IV.5 Summary and conclusions .....210

References .....211

## **Chapter V**

<b>Rational design, synthesis and characterization of Co(II) based MOFs .....</b>	<b>(217-279)</b>
V.1 Introduction .....	219
V.2 Materials and methods .....	242
V.3 Experimental work .....	243
V.3.1 Synthesis .....	243
V.4 Results and discussion .....	248
V.4.1 Structural chemistry and crystal structures of the solids – <b>IITD-25</b> to <b>IITD-33</b> .....	253
V.4.2 Thermogravimetric analysis of new solids – <b>IITD-27</b> , <b>IITD-29</b> and <b>IITD-33</b> .....	271
V.4.3 ATR analysis of new solids – <b>IITD-27</b> , <b>IITD-29</b> and <b>IITD-33</b> .....	271
V.4.4 Hydrogen storage measurements of <b>IITD-27</b> .....	273
V.4.5 Magnetic measurements of <b>IITD-27</b> .....	274
V.5 Summary and Conclusions .....	276
References .....	277
 <b>Chapter VI</b>	
<b>Summary, Conclusions and Future directions .....</b>	<b>(280-284)</b>
 <b>Appendix I</b>	
<b>PXRD analysis of the solids .....</b>	<b>(285-299)</b>

## **Appendix II**

**ATR analysis of the solids .....(300-310)**

**Academic Resume of the author .....(311-314)**

## List of Figures

<b>Figure I.1</b> A pictorial representation of relationship between molecular and crystal synthesis.....	<b>4</b>
<b>Figure I.2</b> A qualitative plot of concentration versus time for the growth of crystals from solution .....	<b>9</b>
<b>Figure I.3</b> Phase diagram of NaCl and water. Three solid phases, ice, NaCl.2H <sub>2</sub> O and NaCl crystallize in this system though the salts occur only above the eutectic composition. Note the salt hydrate could be crystallised only below 0 °C .....	<b>11</b>
<b>Figure I.4</b> The supramolecular aggregation of the tecton {Na(H <sub>2</sub> O) <sub>5</sub> Cl} <sup>0</sup> to form NaCl.2H <sub>2</sub> O.....	<b>12</b>
<b>Figure I.5</b> The hydrocarbon backbone of adamantane-1,3,5,7-tetracarboxylic acid is reduced to a node and O–H•••O interaction is reduced to an edge to form <b>dia</b> topology (bottom left) and its Voronoi polyhedra (bottom right).....	<b>14</b>
<b>Figure I.6</b> Potential applications of metal-organic frameworks.....	<b>16</b>
<b>Figure I.7</b> The construction of MOFs from SBUs and linkers.....	<b>17</b>
<b>Figure I.8</b> Isoreticular series of MOF-5. BDC ligand is replaced by several elongated linkers to produce structures with same topology as MOF-5 ( <b>pcu</b> ) but tuned pore size. However, increasing the length of the linker is limited due to interpenetration.....	<b>19</b>
<b>Figure I.9</b> Isoreticular series of HKUST-1. Different tridentate ligands used to prepare structures with <b>tbo</b> topology similar to HKUST-1.....	<b>20</b>

**Figure I.10** Isoreticular series of Mg-MOF-74. Different dicarboxylate ligands used to prepare structures with **bnn** topology similar to Mg-MOF-74.....21

**Figure I.11** The breaking of bonds in MOF-5 to identify SBU (nodes) to determine topology.....29

**Figure II.1** Supramolecular condensation of the tecton  $\{Zn(sol)_3(BDC)\}$  amongst themselves or with other tectons,  $\{Zn(OH)_2(H_2O)_2\}$  or  $\{Zn(OH)(H_2O)_3\}^+$ ,  $\{Zn(sol)_2(BDC)_2\}^{2-}$  led to all compositions and SBUs observed in the system zinc salt-terephthalic acid-solvent reported in CSD. Red balls represent solvent molecules that would get replaced by carboxylate oxygen. Green and blue balls representing  $-OH$  group and solvent molecules respectively that might or might not get replaced by carboxylate oxygen depending upon the reaction condition. The examples included only those wherein the counter anion of the zinc salt did not compete with terephthalate to coordinate with the metal.....52

**Figure II.2** Zinc solvated complexes present in the solution which could supramolecularly aggregate to form solids that were observable in the structural landscape of the system zinc salt-terephthalic acid-solvent. L represents terephthalate as a complexing ligand. Hydrolysis of the zinc solvated specie to  $\{Zn(sol)_3(OH)\}^+$  or  $\{Zn(sol)_2(OH)_2\}^0$  would occur only when water became a coordinated solvent at supersaturation. The counter anion of the zinc salt, L' was assumed to be in the solution and did not coordinate with the metal.....53

**Figure II.3** Three ways in which 1:1 Zn terephthalate tectons aggregated to form trimeric SBU but with similar composition,  $\{Zn(sol)_{1/1}(BDC)_{3/4}\}_2\{Zn(BDC)_{6/4}\} \equiv [Zn_3(sol)_2(BDC)_3]$ . The numerator denotes the number of ligands coordinated to zinc and the denominator refers to the number of zinc atoms a ligand is linked to.....55

**Figure II.4** Type C (trimeric SBU) extending into third dimension in BADZAK, KOZNEU, KOZNIY by suitably condensing with either the ion-pairs,  $\{\text{Me}_2\text{NH}_2\}_2[\text{BDC}]$ ,  $\{\text{Me}_2\text{NH}_2\}[\text{HCOO}]$  or another complex  $\{\text{Zn}(\text{sol})_4(\text{HCOO})_2\}$  respectively.....**56**

**Figure II.5** Bond distances in ORIBAU (top) and SERKOQ (bottom) confirming that BDC were dianions and the framework is  $\{\text{Zn}_3(\text{BDC})_4\}^{2-}$ . The formulae proposed in the original papers were incorrect.....**57**

**Figure II.6** Four molecules of the type  $\{\text{Zn}(\text{sol})_4(\text{BDC})\}$  resulted in a dimeric SBU with the composition  $\{\text{Zn}(\text{sol})(\text{BDC})_{4/4}\}_2 \equiv \{\text{Zn}_2(\text{sol})_2(\text{BDC})_2\}$ . AFOSIY, DAXNOG, GECXUH, HIQVUZ, SATFEZ have similar aggregation pattern but with different coordinated solvent. In GECXUH, the presence of water as part of zinc tecton,  $\{\text{Zn}(\text{sol})_3(\text{H}_2\text{O})(\text{BDC})\}$  resulted in a dimeric SBU with the composition  $\{\text{Zn}(\text{H}_2\text{O})(\text{BDC})_{4/4}\}_2 \equiv \{\text{Zn}_2(\text{H}_2\text{O})_2(\text{BDC})_2\}$ .....**60**

**Figure II.7** A rare example wherein the supramolecular aggregation of the tecton  $\{\text{Zn}(\text{H}_2\text{O})_4(\text{BDC})\}$  was not restricted to dimeric unit as in aprotic solvents but resulted in a 3D coordinated zinc terephthalate,  $\{\text{Zn}(\text{H}_2\text{O})(\text{BDC})_{4/4}\} \equiv \{\text{Zn}(\text{H}_2\text{O})(\text{BDC})\}$  in IFABIA and 1D chain,  $\{\text{Zn}(\text{H}_2\text{O})_2(\text{BDC})_{2/2}\} \equiv \{\text{Zn}(\text{H}_2\text{O})_2(\text{BDC})\}$  in DIKQET. The unusual assembly was probably triggered by a strong H-bonding exerted by the presence of coordinated water molecules.....**61**

**Figure II.8** The substitution of solvent molecules by water in the coordination sphere of the tecton has another effect. Under suitable condition, it underwent hydrolysis. At this stage, the aggregation of zinc terephthalate competed with another tecton,  $\{\text{Zn}(\text{H}_2\text{O})_3(\text{OH})_2\}$ . The aggregation of the two tectons,  $\{\text{Zn}(\text{sol})_4(\text{BDC})\}$  and  $\{\text{Zn}(\text{H}_2\text{O})_3(\text{OH})_2\}$  in 1:1 molar ratio resulted in PUCYAO while the molar ratio 3:2 led to REDROI.....**62**

<b>Figure II.9</b> The aggregation of the tecton, $\{\text{Zn}(\text{H}_2\text{O})_2(\text{OH})_2\}$ in ZnO (wurtzite structure) .....	<b>63</b>
<b>Figure II.10</b> The aggregation of the three tectons, $\{\text{Zn}(\text{sol})_3(\text{BDC})\}$ , $\{\text{Zn}(\text{sol})_2(\text{BDC})_2\}^{2-}$ , and $\{\text{Zn}(\text{H}_2\text{O})_3(\text{OH})\}^+$ in 1:1:2 molar ratio results in SAHYOQ.....	<b>65</b>
<b>Figure II.11</b> The aggregation of tecton, $\{\text{Zn}(\text{H}_2\text{O})_4(\text{HCOO})_2\}$ and the ion-pair $\{\text{Me}_2\text{NH}_2\}[\text{HCOO}]$ led to a 3D solid with the composition $\{\text{Me}_2\text{NH}_2\}[\text{Zn}(\text{HCOO})_{6/2}] \equiv \{\text{Me}_2\text{NH}_2\}[\text{Zn}(\text{HCOO})_3]$ . The solid is the same as DAXNIA04.....	<b>66</b>
<b>Figure II.12</b> The aggregation of tecton, $\{\text{Zn}(\text{H}_2\text{O})_4(\text{HCOO})_2\}$ amongst themselves result in three dimensional solid with zinc in two coordination environments. $[\text{Zn}(\text{HCOO})_{6/2}][\text{Zn}(\text{H}_2\text{O})_{4/1}(\text{HCOO})_{2/2}] \equiv [\text{Zn}(\text{H}_2\text{O})_4(\text{HCOO})_4]$ . The solid is identical to ZNFORD06.....	<b>68</b>
<b>Figure II.13</b> The aggregation pattern in QUGWEW.....	<b>70</b>
<b>Figure II.14</b> The aggregation pattern of NUKCEC.....	<b>71</b>
<b>Figure II.15</b> The aggregation pattern of EBIPOX.....	<b>71</b>
<b>Figure II.16</b> The aggregation of the two tectons $[\text{Zn}(\text{sol})_3(\text{BDC})]$ and $[\text{Na}(\text{sol})_5(\text{BDC})]$ leads to the formation of HUTZEB and ISORAJ.....	<b>72</b>
<b>Figure II.17</b> The aggregation of the two tectons $[\text{Zn}(\text{sol})_2(\text{NMe}_2)(\text{BDC})]$ and $[\text{Na}(\text{sol})_5(\text{Me}_2\text{NH}_2)(\text{BDC})]$ results in XIRHUC.....	<b>72</b>
<b>Figure II.18</b> Topological representation of the solids; AFOSIY, AFOSOE and BADZAK.....	<b>74</b>

**Figure II.19** Topological representation of the solids; IFABIA, SAHYOQ and PUCYAO.....75

**Figure III.1** Crystal engineering of zinc imidazole (or N-derivatives) based 0D (molecular solid) and 1D structures. The cartoon schematically describes how different stoichiometries of soluble zinc imidazole complexes coordinate with X (single donor or multiple donor or chelate) and eventually condense to nucleate 0D or 1D solids. REFCODEs refer to the examples available in CSD.....85

**Figure III.2** The aggregation of  $[\text{Zn}(\text{sol})_3(\text{RIm})]$  or  $[\text{Zn}(\text{sol})_4(\text{RIm})]$  with coordinating anions leading to 0D, 1D, 2D structures.....87

**Figure III.3** The aggregation of  $[\text{Zn}(\text{sol})_2(\text{RIm})_2]$  with coordinating anions leading to 0D or 1D structures.....87

**Figure III.4** The aggregation of  $[\text{Zn}(\text{sol})_2(\text{RIm})_3]$  with dicarboxylate leading to 1D and the aggregation of  $[\text{Zn}(\text{sol})_2(\text{RIm})_4]$  leading to 0D structures.....88

**Figure III.5** The representation of phosphate derivatives leading to multi-dimensional structures.....89

**Figure III.6** The cartoon shows how the geometry of soluble zinc imidazole aromatic carboxylate  $\{\text{Zn}(-\text{COO})_2(\text{RIm})_2(\text{sol})\}$  (tecton) influences supramolecular aggregation and hence the final condensed structure of solids with different extended coordination linkage.....90

**Figure III.7** Crystal structure of **IITD-1**. Supramolecular aggregation of the tecton  $\{\text{Zn}(\text{HIm})(\text{BDC})(\text{sol})_2\}$  condensing into 2D sheets where imidazole blocks the extension of coordination into the third dimension.  $\text{N}-\text{H}\cdots\text{O}$  interactions facilitate packing of 2D sheets.

The SBU,  $\{Zn_2(HIm)_2(COO_{BDC})_2(COO_{BDC'})_2\}$  leads to four-connected uninodal net with sql topology and point symbol  $\{4^4.6^2\}$ .....**110**

**Figure III.8** Crystal structure of **IITD-2**. Supramolecular aggregation of the 1:1 tecton  $\{Zn(sol)(HIm)_2(BDC)\}$  condensing into 1D chains. The two imidazoles attached to zinc restrict BDC to extend only in one direction leading to 1D chains. N–H···O interactions facilitate packing of 1D chains. The SBU in **IITD-2**,  $\{Zn(HIm)_2(COO_{BDC})_2\}$  results in a 4-c uninodal net with dia topology and point symbol  $\{6^6\}$ .....**111**

**Figure III.9** Crystal structure of **IITD-3**. Supramolecular aggregation of the tecton,  $\{Zn(sol)_3(BDC)\}$  and the ion-pair, two  $\{Me_2NH_2\}^+$ , BDC and two water molecules condensing to form 3D coordination network. The SBU,  $\{Zn_3(COO_{BDC})_2(COO_{BDC'})_2(COO_{BDC''})_4\}$  is node1 and the linker is an edge. **IITD-3** shows 8-connected uninodal net with point symbol  $\{3^6.4^4.5^7.6\}$ .....**113**

**Figure III.10** Crystal structure of **IITD-4**. The tecton,  $\{Zn(sol)_3(BDC)\}$  condenses with  $\{Zn(sol)_4(OH)_2\}$  in the molar ratio 3:1 condensing into a 3D interpenetrated structure. The SBU,  $\{Zn_4(DMSO)_4(COO_{BDC})_4(COO_{BDC'})_2(OH)_2\}$  is node1 and 2-c phenyl ring is an edge. It is a 6-connected uninodal net with interpenetrated pcu topology and point symbol  $\{4^{12}.6^3\}$ .....**115**

**Figure III.11** Crystal structure of **IITD-5**. Supramolecular aggregation of the tecton  $\{Zn(HIm)_2(1,4-PDA)(sol)\}$  analogous to the one observed in **IITD-2** condensing into 1D chains. N–H···O interactions facilitating the packing of 1D chains is different from **IITD-2**. Its 3D supramolecular structure shows a new topology with six-connected uninodal net and point symbol  $\{4^6.5^3.6^6\}$ .....**116**

**Figure III.12** Crystal structure of **IITD-6**. Supramolecular aggregation of the tecton  $\{\text{Zn(sol)}(\text{HIm})_2(2,6\text{-NDC})\}$  analogous to the ones observed in **IITD-2** and **IITD-5** condensing into 1D chains. N–H···O interactions facilitate the packing of 1D chains but different from **IITD-2** and **IITD-5**. The 3D supramolecular structure of **IITD-6** shows a different topology with six-connected uninodal net and point symbol  $\{4^8.6^7\}$ .....**118**

**Figure III.13** Crystal structure of **IITD-7**. Supramolecular aggregation of the tecton  $\{\text{Zn}(\text{HIm})_2(4,4'\text{-OBB})(\text{sol})\}$  condensing into 1D chains. N–H···O interactions facilitate packing of 1D chains with a new topology with eight-connected uninodal net and point symbol  $\{3^3.4^2.5.6^2\}$ .....**120**

**Figure III.14** Crystal structure of **IITD-8**. Supramolecular aggregation of the tecton  $\{\text{Zn(sol)}_3(4,4'\text{-SDC})\}$  forming a Type A trimer finally leading to two-dimensional sheet. **IITD-8** shows 6-connected uninodal net with hxl topology and point symbol  $\{3^6.4^6.5^3\}$ .....**122**

**Figure III.15** Thermograms of solids– concomitant mixture of **IITD-1** and **IITD-2**, **IITD-5** and **IITD-6**. .....**123**

**Figure IV.1** Various binding modes of triazole and triazolates.....**133**

**Figure IV.2** Formation of two-dimensional sheet in NOKPAF, UQETAN and XAPNUZ.....**136**

**Figure IV.3** Formation of two-dimensional sheet in FAMFAC and UGUJOW.....**137**

**Figure IV.4** CSD analysis of zinc/cadmium triazolates or zinc/cadmium triazolate dicarboxylate based compounds.....147

**Figure IV.5** Binding modes of 2,5-dihydroxyterephthalate in **IITD-9** to **IITD-13** where (1) represents bidentate syn-mode and (2) represents monodentate anti-mode.....168

**Figure IV.6** Crystal structure of **IITD-9**; a pillared layer structure formed from cadmium triazolate layer (left) viewed along [100] being connected by dicarboxylate linker to form final 3D structure of **IITD-9**. A plausible supramolecular pathway showing how the PZC, a cadmium dimer of the composition,  $\{\text{Cd}_2(\text{Trz})_2(\text{DHTP})(\text{sol})_6\}^0$  condense with each other to maximise coordination interaction leading to **IITD-9**,  $[\text{Cd}_2(\text{Trz})_2(\text{DHTP})(\text{DMF})_2]$  .....169

**Figure IV.7** The monomeric Cd complex with DHTP with the composition,  $\{\text{Cd}(\text{DHTP})(\text{sol})_5\}^0$  is considered as the PZC. These PZCs condense together to form 1D chains. The two coordinated water molecules facilitate H-bonding between the chains and methyl groups of DMSO show C–H...C with the aromatic phenyl ring and C–H...O with carboxylate oxygen finally forming the supramolecular structure of **IITD-12**,  $[\text{Cd}(\text{DHTP})(\text{H}_2\text{O})_2]$  viewed along [100] .....170

**Figure IV.8** The monomeric Cd complex with DHTP (the PZC) with the composition,  $\{\text{Cd}(\text{DHTP})(\text{sol})_4\}^0$  condenses with similar PZCs to form zig zag chains viewed along [001] and [010]. The two coordinated water molecules facilitate H-bonding between the chains on the (010) and (001) finally forming the supramolecular structure of **IITD-13**,  $[\text{Cd}(\text{DHTP})(\text{H}_2\text{O})_2]$  viewed along [100] .....172

**Figure IV.9** Binding modes of 5-aminoisophthalic acid in **IITD-14** to **IITD-16**.....173

**Figure IV.10** A cadmium dimer  $\{\text{Cd}_2(\text{Trz})_2\}^{2+}$  aggregates with AIP to form PZC  $\{\text{Cd}_2(\text{Trz})_2(\text{AIP})(\text{sol})_6\}^0$  which further aggregate together (right) resulting in **IITD-14**. The ball and stick and polyhedral representation of **IITD-14** (left) is without solvent molecules. The pores inside the framework (left) are filled with AIP and DMF in the final structure of **IITD-14** (right).....174

**Figure IV.11** Two crystallographically different  $\{\text{Cd}_2(\text{Trz})_2(\text{AIP})(\text{sol})_6\}$  combined to form the tecton with the composition  $\{\text{Cd}_4(\text{Trz})_4(\text{AIP})_2(\text{sol})_{11}\}^0$ . The condensation of these tectons led to the extended framework of **IITD-15** (right). The ball and stick and polyhedral representation of **IITD-15** without solvent molecules and AIP show pores inside the framework (left) which are filled in the final structure of **IITD-15** with DMF and AIP (right). .....176

**Figure IV.12** Three PZCs  $\{\text{Cd}(\text{AIP-NH}_2)(\text{sol})_6\}^0$ ,  $\{\text{Cd}(\text{AIP-COO})(\text{sol})_6\}^0$ ,  $\{(\text{Me}_2\text{NH}_2)_2(\text{AIP})\}^0$  condensed to form **IITD-16**.....177

**Figure IV.13** Binding modes of benzenedicarboxylic acid in **IITD-17– IITD-21**.....178

**Figure IV.14** Crystal structure of **IITD-17**. The aggregation of 1:1 Cd:BDC complex led to the growth of **IITD-17** with composition  $[\text{Cd}(\text{BDC})(\text{DMSO})]$  .....179

**Figure IV.15** Crystal structure of **IITD-18**. The aggregation of 1:1 Cd:BDC complex led to the growth of **IITD-18** with composition  $[\text{Cd}(\text{BDC})(\text{H}_2\text{O})]$  .....180

**Figure IV.16** Crystal structure of **IITD-19**. Supramolecular condensation of two soluble cadmium PZC,  $\{\text{Cd}(\text{Trz})_2(\text{sol})_4\}$  and  $\{\text{Cd}(\text{BDC})(\text{sol})_5\}$  forming **IITD-19** with the composition  $[\text{Cd}_2(\text{Trz})_2(\text{BDC})(\text{DMSO})_2]$ . The assembly facilitates a cadmium dimer through adjacent

nitrogens of triazolate while the third nitrogen extends the coordination with cadmium of adjacent dimers.....182

**Figure IV.17** Crystal structure of **IITD-20**. The supramolecular aggregation of the tectons  $\{\text{Cd}_2(\text{trz})_2(\text{BDC})_2(\text{sol})_4\}^{2-}$  and  $\{\text{Cd}(\text{sol})_6\}^{2+}$  forms PZC with composition  $\{\text{Cd}_3(\text{trz})_2(\text{BDC})_2(\text{sol})_9\}^0$  which further aggregates with another to form **IITD-20** with composition  $\{\text{Cd}_3(\text{trz})_2(\text{BDC})_2(\text{DMSO})_5\}$ .....183

**Figure IV.18** Crystal structure of **IITD-21**. The supramolecular aggregation of the tectons  $\{\text{Cd}_2(\text{Trz})_2(\text{BDC})_2(\text{sol})_4\}^{2-}$  and  $\{\text{Cd}(\text{sol})_6\}^{2+}$  to form a PZC  $\{\text{Cd}_3(\text{Trz})_2(\text{BDC})_2(\text{sol})_9\}$  which further aggregates with another to form **IITD-21** with composition  $\{\text{Cd}_3(\text{Trz})_2(\text{BDC})_2(\text{DMSO})_2(\text{H}_2\text{O})_2\}$  (c). (d) represents the final porous structure of the **IITD-21**; pores are filled with DMSO.....185

**Figure IV.19** Crystal structure of **IITD-22**. The tecton  $\{\text{Cd}_2(\text{Trz})(\text{sol})_{10}\}$  combines with BTC to form PZC  $\{\text{Cd}_2(\text{trz})(\text{BTC})(\text{sol})_8\}$ . These PZCs further aggregate with one another via supramolecular interactions to construct the final structure of **IITD-22** with composition  $[\text{Cd}_2(\text{trz})(\text{BTC})(\text{DMF})(\text{H}_2\text{O})]$  .....186

**Figure IV.20** Crystal structure of **IITD-23**. (a) Coordination environment of cadmium. (b) Supramolecular condensation of the PZC  $\{\text{Cd}_2(\text{Trz})_2(\text{FDA})(\text{sol})_6\}$  into final crystal structure of **IITD-23**; pores are filled with DMF (c) and empty pores when solvents are removed (d) .....188

**Figure IV.21** Crystal structure of **IITD-24**. (a) Coordination environment of cadmium. (b) Supramolecular aggregation of the PZC,  $\{\text{Cd}_2(\text{Trz})_2(\text{TDA})(\text{sol})_6\}$  condensing into the

framework. Pores are filled with DMF. (c) Structure of the coordination framework with the removal of solvents from the pores.....189

**Figure IV.22** Thermograms of the solids – **IITD-9** to **IITD-13**.....192

**Figure IV.23** Thermograms of the solids – **IITD-14** to **IITD-16**.....193

**Figure IV.24** Thermograms of the solids – **IITD-17**, concomitant mixture of **IITD-17** & **IITD-20**, **IITD-22**, **IITD-23** and **IITD-24**.....194

**Figure V.1** (a) The soluble discrete complex species (tectons),  $\{\text{Co}^{\text{II}}(\text{H}_2\text{BTC})_2(\text{H}_2\text{O})_4\}$  supramolecularly aggregate through H-bonding between coordinated water and carboxylate oxygen to form 0D **IITD-25**. In (c)-(f), H-bonding interactions involved in crystal packing are shown.....254

**Figure V.2** (a) An unusual 1D chain formed from two sets of tectons: The soluble species  $\{\text{Co}^{\text{I}}(\text{H}_2\text{O})_6\}^{2+}$  and  $\{\text{Co}^{\text{II}}(\text{BTC})(\text{H}_2\text{O})_5\}^-$  condense in the molar ratio 1:2 forming the chain of the composition,  $\{\text{Co}^{\text{I}}(\text{H}_2\text{O})_4(\text{BTC})_{2/2}\}_2\{\text{Co}^{\text{II}}(\text{H}_2\text{O})_4(\text{BTC})_{1/1}(\text{BTC}')_{1/1}\} \equiv [\text{Co}^{\text{II}}_3(\text{BTC})(\text{H}_2\text{O})_{12}]$ . Note how the system optimises the stoichiometry between the divalent cobalt and trivalent BTC. The adjacent chains are further stabilized through O–H•••O between coordinated water molecules and carboxylate oxygens ((c)&(d)) .....255

**Figure V.3** (a) Coordination environment of Co(II), HTrz and HBTC in **IITD-27**. (b) The soluble 1:1 complex,  $\{\text{Co}^{\text{II}}(\text{HTrz})(\text{HBTC})(\text{sol})_4\}$  aggregates in such a way resulting in helical 1D chains bridged through the second carboxylate of HBTC forming a 3D coordination framework in **IITD-27**; the third carboxylic acid of HBTC involves only in H-bonding interaction. The 1D helical chain (c) is extended into the other two dimensions via HBTC in (d) &(e) to form **IITD-**

27 with composition  $\{\text{Co}(\text{HTrz})_{2/2}(\text{HBTC})_{3/3}(\text{H}_2\text{O})\} \equiv [\text{Co}(\text{HTrz})(\text{HBTC})(\text{H}_2\text{O})]$   
 (f).....257

**Figure V.4** (a) The hexameric wheel of  $\{\text{Co}_6(\text{HCOO})_6(\text{BTC})_6\}$  in **IITD-28** and its (b) polyhedral representation. (c) Supramolecular condensation of the two PZCs  $\{\text{Co}_2(\text{BTC})(\text{HCOO})(\text{sol})_8\}$  and  $\{\text{Co}(\text{HCOO})_2(\text{sol})_4\}$  resulting in the formation of 2D sheet of **IITD-28** with the composition  $[\text{Co}^{\text{II}}_3(\text{HCOO})_3(\text{BTC})(\text{DMF})_3]$  shown in (d). Note how formate and the three carboxylates in BTC bridge adjacent  $\text{Co}^{\text{II}}$  ions.....259

**Figure V.5** (a) An unusual trimeric cluster,  $\{\text{Co}^{\text{II}}_3(\text{HTrz})_2(\text{BTC})_2\}$  in **IITD-29** arising from the condensation two molecules of  $\{\text{Co}(\text{BTC})(\text{sol})_5\}^-$  and one molecule of  $\{\text{Co}(\text{HTrz})_2(\text{sol})_4\}^{2+}$  as shown in (b). The discrete trinuclear cobalt cluster is further stabilised through H-bonding interactions as shown in (c)-(e) .....260

**Figure V.6** (a) shows the crystal structure of **IITD-30** and the supramolecular condensation of the soluble 1:2 complex specie,  $\{\text{Co}(5\text{-HAIP})_2(\text{H}_2\text{O})_4\}$  facilitating 2D sheet in **IITD-30** (c) with the composition  $\{\text{Co}(5\text{-HAIP})_{4/2}(\text{H}_2\text{O})_{2/1}\} \equiv [\text{Co}(5\text{-HAIP})_2(\text{H}_2\text{O})_2]$ . Note one carboxylate is not extending the metal.....262

**Figure V.7** (a) and (c) represents the ball and stick and polyhedral representation of **IITD-31**. (b) shows the aggregation of PZC  $\{\text{Co}(5\text{-AIP})(\text{sol})_4\}$  to form one-dimensional chain in **IITD-31**  $[\text{Co}(5\text{-AIP})(\text{H}_2\text{O})_2]$  .....263

**Figure V.8** (a) Coordination environment around cobalt(II) and BDC anion. (b) Supramolecular assembly of the 1:1 tecton,  $\{\text{Cd}(\text{BDC})(\text{sol})_5\}$  **IITD-32**. (c) and (d) depicts the ball and stick and polyhedral representation of the condensed structure **IITD-32** with the composition,  $\{\text{Co}(\text{sol})_2(\text{BDC})_{4/4}\} \equiv [\text{Co}(\text{BDC})(\text{H}_2\text{O})]$  .....265

**Figure V.9** (a) Coordination environment of Co(II), HTrz and BDC in **IITD-32**. (b) Supramolecular condensation of soluble 1:1 complex,  $\{\text{Co}^{\text{II}}(\text{BDC})(\text{sol})_4\}$  with  $\{\text{Co}^{\text{II}}(\text{HTrz})(\text{Trz})_2(\text{sol})_3\}$  in **IITD-33**. The 2D cadmium triazolate layer ((c) & (d)) extending into 3D coordination framework via BDC (e). The composition of the pillared-layer is  $\{\text{Co}_1(\text{Trz})_{4/3}(\text{HTrz})_{2/2}\} \quad \{\text{Co}_2(\text{Trz})_{2/3}(\text{BDC})_{2/2}\} \quad \equiv \{\text{Co}_2(\text{Trz})_{6/3}(\text{HTrz})_{2/2}(\text{BDC})_{2/2}\} \equiv [\text{Co}_2(\text{Trz})_2(\text{HTrz})(\text{BDC})]$ .....**266**

**Figure V.10** Thermograms of the solids– **IITD-17**, **IITD-29** and **IITD-33**.....**272**

**Figure V.11** Excess hydrogen uptake capacity in **IITD-27** at 77 and 303K.....**273**

**Figure V.12** In-situ raman study of adsorbed hydrogen in **IITD-27** at different temperatures.....**274**

**Figure V.13** (a)  $\chi_M$  versus T plot and (b)  $\chi_M^{-1}$  versus T plots in the range 5-300K at 1000Oe (or 0.1Tesla) for **IITD-27**.....**275**

## List of Tables

<b>Table I.1</b> Molecular synthesis versus crystal synthesis .....	<b>5</b>
<b>Table I.2</b> Selected noncovalent interactions .....	<b>7</b>
<b>Table I.3</b> Properties of hydrogen bonds .....	<b>7</b>
<b>Table II.1</b> REFCODEs and composition of all zinc terephthalate with or without competing counter anions crystallizing from solution containing zinc solvate/hydrate complex and terephthalate reported in CSD.....	<b>48</b>
<b>Table III.1</b> CCDC refcodes and composition of the solids containing Zn and imidazole. The dimensionality of the metal-ligand (dicarboxylate or counter ion, X) coordination linkage into 0D (molecular solid) or 1D, 2D or 3D (nonmolecular) .....	<b>92</b>
<b>Table III.2</b> CCDC refcodes and composition of the solids containing Zn and N-derivative of imidazole.....	<b>97</b>
<b>Table III.3</b> CCDC refcodes and composition of the solids containing Zn and imidazolate.....	<b>102</b>
<b>Table III.4</b> Crystallographic details of the solids – <b>IITD-1</b> to <b>IITD-8</b> .....	<b>124</b>
<b>Table III.5</b> Selected bond distances (Å) and angles (°) of the new solids – <b>IITD-2</b> , <b>IITD-5</b> and <b>IITD-6</b> .....	<b>126</b>
<b>Table IV.1</b> CCDC Refcodes and compositions of zinc triazolate mono/dicarboxylates.....	<b>138</b>
<b>Table IV.2</b> CCDC Refcodes and compositions of cadmium triazolate mono/dicarboxylates.....	<b>141</b>

<b>Table IV.3</b> Classification of Zn/Cd-HTrz/Trz-mono/dicarboxylate.....	<b>146</b>
<b>Table IV.4</b> Cell parameters of the solids ( <b>IITD-9</b> to <b>IITD-24</b> ) synthesized via different reaction conditions.....	<b>160</b>
<b>Table IV.5</b> Crystallographic details of the solids– <b>IITD-9</b> to <b>IITD-24</b> .....	<b>196</b>
<b>Table IV.6</b> Selected bond angles(°) and distances(Å)– <b>IITD-9</b> to <b>IITD-24</b> .....	<b>202</b>
<b>Table V.1</b> CCDC Refcodes and composition of the solids containing cobalt(II) and imidazole.....	<b>221</b>
<b>Table V.2</b> CCDC Refcodes and composition of the solids containing cobalt and N-derivative of imidazole (Im(d)) .....	<b>228</b>
<b>Table V.3</b> CCDC Refcodes and composition of the solids containing Co and imidazolate.....	<b>237</b>
<b>Table V.4</b> CCDC Refcodes and composition of the solids containing Co(II) and triazole, N-derivatives of triazole and triazolate.....	<b>238</b>
<b>Table V.5</b> Summary of results obtained from single crystal analysis under different reaction conditions.....	<b>249</b>
<b>Table V.6</b> Crystallographic details of the solids– <b>IITD-25</b> to <b>IITD-33</b> .....	<b>267</b>
<b>Table V.7</b> Selected bond distances(Å) and angles (°) of the solids, <b>IITD-25</b> , <b>IITD-29</b> and <b>IITD-33</b> .....	<b>270</b>

## List of schemes

<b>Scheme III.1</b> Synthetic protocol employed for the solids– <b>IITD-1</b> to <b>IITD-8</b> .....	<b>105</b>
<b>Scheme IV.1</b> A schematic representation of the system zinc salt-triazole-dicarboxylic acid, where zinc triazolate layers are pillared through dicarboxylate linkers. The label of the organic linkers corresponds to the REFCODEs of the compounds reported in CSD.....	<b>135</b>
<b>Scheme IV.2</b> A crystal engineering strategy to design cadmium triazolate chains (1D) to layers (2D) to finally pillared-layer structures (3D) .....	<b>142</b>
<b>Scheme IV.3</b> A crystal engineering strategy to tune the dimensionality of the coordination linkage of the cadmium triazole/triazolate carboxylate-based solids by appropriately choosing organic linkers.....	<b>145</b>
<b>Scheme IV.4</b> Reaction scheme for the synthesis of the solids – <b>IITD-9</b> to <b>IITD-24</b> .....	<b>148</b>
<b>Scheme IV.5</b> Structural landscape of cadmium triazolate 2,5-dihydroxyterephthalate and cadmium triazolate 5-aminoisophthalate ( <b>IITD-9</b> to <b>IITD-16</b> ) .....	<b>149</b>
<b>Scheme V.1</b> Synthetic protocol followed to prepare <b>IITD-25</b> to <b>IITD-27</b> .....	<b>245</b>
<b>Scheme V.2</b> Synthetic protocol followed to prepare <b>IITD-30</b> and <b>IITD-31</b> .....	<b>246</b>
<b>Scheme V.3</b> Synthetic protocol followed to prepare <b>IITD-32</b> and <b>IITD-33</b> .....	<b>247</b>

## Abbreviations

CSD – Cambridge Structural Database

CCDC – Cambridge Crystallographic Data Centre

DMF – dimethylformamide

DMA – dimethylacetamide

DMSO – dimethylsulphoxide

HIm – imidazole

Im – imidazolate

HTrz – triazole

Trz – triazolate

Sol – solvent

H<sub>2</sub>BDC – benzene-1,4-dicarboxylic acid

BDC – benzene-1,4-dicarboxylate/ terephthalate

1,2-BDC – benzene-1,2-dicarboxylate

2-NH<sub>2</sub>BDC – 2-aminobenzene-1,4-dicarboxylate

2-BrBDC – 2-bromobenzene-1,4-dicarboxylate

2-HOBDC – 2-hydroxybenzene-1,4-dicarboxylate

2,5-(HO)<sub>2</sub>BDC – 2,5-dihydroxybenzene-1,4-dicarboxylate

2,5-(NH<sub>2</sub>)<sub>2</sub>BDC – 2,5-diaminobenzene-1,4-dicarboxylate

2,3,5,6-(F)<sub>4</sub>-BDC – 2,3,5,6-tetrafluorobenzene-1,4-dicarboxylate

IP – isophthalate

5-NH<sub>2</sub>-IP – 5-aminoisophthalate

5-<sup>t</sup>butyl-IP – 5-<sup>t</sup>butylisophthalate


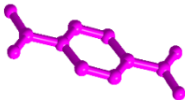

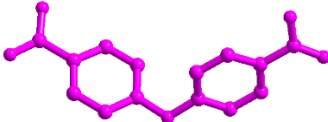

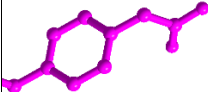

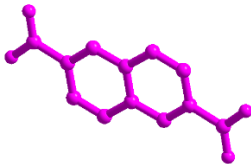



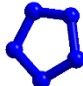



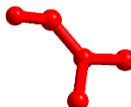

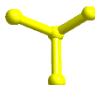

5-SO<sub>2</sub>IP – 5-sulfoisophthalate

5-NO<sub>2</sub>IP – 5-nitroisophthalate

1,3,5-BTC – 1,3,5-benzenetricarboxylate  
1,4-NDC – naphthalene-1,4-dicarboxylate  
2,6-NDC – naphthalene-2,6-dicarboxylate  
1,4-PDA – phenylene 1,4-diacetate  
4,4'-OBB – 4,4'-oxybisbenzoate  
2,5-FDC – 2,5-furandicarboxylate  
2,5-TDC – 2,5-thiophenedicarboxylate  
4,4'-SDC – 4,4'-stilbene dicarboxylate  
4,4'-BPDC – 4,4'-biphenyldicarboxylate  
4,4'-SDBA – 4,4'-sulfonyldibenzoate  
2,6-Me<sub>2</sub>-PyDC – 2,6-dimethylpyridine-3,5-dicarboxylate  
Ox – oxalate  
Suc – succinate  
Tar – tartarate  
Glu – Glutarate  
Adi – adipate  
HMPH – homophthalate  
4-CMB – 4-carboxymethylbenzoate  
4-CEB – 4-(2-carboxyethyl)benzoate  
1,3,5,7-H<sub>2</sub>ADTC – adamantane-1,3,5,7-tetracarboxylic acid  
BPYDB – 4-(6-(4-carboxylatophenyl)-4,4'-bipyridin-2-yl)benzoate  
TTBDC – trans,trans-1,3-butadiene-1,4-dicarboxylate  
4,4'-HFIPBB – 4,4'-(1,1,1,3,3,3-hexafluoropropane-2,2-diyl)dibenzoate  
DBTDC – 5,5-dioxo-5H-dibenzo[b,d]thiophene-3,7-dicarboxylate  
DFBPDC – 2,2'-difluoro[1,1'-biphenyl]-4,4'-dicarboxylate

DTTDC – dithieno-[3,2-*b*;2',3'-*d*]-thiophene-2,6-dicarboxylate

### Color codes of atoms/ligands used in this work

	Sodium (Na)		Terephthalic acid
	Zinc (Zn)		Oxybisbenzoic acid
	Copper (Cu)		Phenylenediacetic acid
	Magnesium (Mg)		Naphthalene dicarboxylic acid
	Cadmium (Cd)		Stilbenedicarboxylic acid
	Cobalt (Co)		Imidazole
	Oxygen (O)		Dimethylammonium cation
	Nitrogen (N)		DMF
	Carbon (C)		DMSO
	Sulfur (S)		